Vertical kinematics of the thick disc at $4.5 \lesssim R \lesssim 9.5$ kpc

Kohei Hattori[1]* and Gerard Gilmore[1]

[1]*Institute of Astronomy, University of Cambridge, Madingley Road, Cambridge CB3 0HA, United Kingdom*

ABSTRACT

We explored a method to reconstruct the distribution function of the Galactic thick disc within the action space where nearby thick-disc stars are distributed. By applying this method to 127 chemically-selected thick-disc stars in the Solar neighbourhood, we found that the vertical velocity dispersion that corresponds to the reconstructed distribution function declines approximately as $\exp(-R/R_s)$ at $4.5 \text{ kpc} \lesssim R \lesssim 9.5 \text{ kpc}$, with $R_s = 8.3 \pm 1.1(\text{rand.}) \pm 1.6(\text{sys.})$ kpc. Also, we found that the vertical velocity dispersion σ_z of our local thick-disc stars shows only weak dependency on radial and azimuthal velocities (v_R, v_ϕ). We discuss possible implications of these results on the global structure of the Milky Way thick disc.

Key words: – Galaxy: disc – Galaxy: evolution – Galaxy: formation – Galaxy: kinematics and dynamics – Galaxy: structure – solar neighbourhood

1 INTRODUCTION

Historically, the thick disc of the Milky Way was first identified through star counts toward the Galactic Poles as a vertically extended disc component with scale height ~ 1 kpc (Yoshii 1982; Gilmore & Reid 1983), in addition to the thin disc with scale height ~ 0.3 kpc that dominates the disc stars in the immediate Solar neighbourhood. Therefore, at the outset, the tentative definition of the thick-disc stars was those disc stars with large vertical orbital excursions and large vertical velocities.

Later, spectroscopic studies (e.g., Bensby et al. 2003, 2004; Reddy et al. 2006) on kinematically-selected disc stars suggested that stars with large vertical motions (which are likely to belong to the thick disc) tend to show lower [Fe/H] and higher [α/Fe] than those with small vertical motions (thin-disc stars). These chemical properties suggest that the thick-disc stars are older than thin-disc stars (lower [Fe/H]) and that the star formation timescale of the thick disc was shorter than that of the thin disc (higher [α/Fe]).

Recently, Klaus Fuhrmann (Fuhrmann 1998, 2004, 2008, 2011) investigated a kinematically-unbiased volume-complete sample of Solar-type disc and halo stars located within 25 pc of the Sun. The distribution of his sample stars in the [Fe/H]-[Mg/Fe] space reveals two chemically distinct populations of disc stars (see Figure 15 of Fuhrmann 2011). Based on the kinematical properties of these populations, he identified the lower-[Fe/H] and higher-[Mg/Fe] population to be the thick disc, and the other population to be the thin disc. This clear separation between the thin

and thick discs is also confirmed in the nearby (heliocentric distance $d < 100$ pc) kinematically-unbiased sample of Adibekyan et al. (2012) for which [Fe/H] and [α/Fe] are available through high-resolution spectroscopy. These recent observations suggest that the thick disc is better defined by chemical compositions of stars, especially by [Fe/H] and [α/Fe] (Masseron & Gilmore 2015).

In the past decades, our understanding of the structure of the thick disc towards the Galactic Poles has been greatly improved (Gilmore et al. 1989; Rix & Bovy 2013; Yoshii 2013). The next step forward is to unravel its more global structure, such as the radial dependence of its vertical structure. So far, many attempts have been made to fulfil this goal, and they are broadly categorised into two classes of studies.

The first class of studies are based on nearby samples of disc stars. One such example is Binney (2012), who fitted the distribution of local disc stars with his distribution function model. He discussed some global structure of the thick disc by looking into his best-fit models. Although this kind of studies can predict almost everything if the best-fit models are reasonably correct, one critical problem with these studies is the validity of the functional forms of the assumed distribution functions.

The second class of studies are based on in-situ samples of (relatively) distant disc stars. This class can be further categorised into three sub-classes: those studies using (i) high-resolution spectroscopic samples; (ii) medium-resolution spectroscopic samples; or (iii) photometric samples. The advantage of sub-class (i) studies is that we can define the thick disc purely by means of the stellar chemistry (Bensby et al. 2011). However, the number of stars that are

---

* E-mail: khattori@ast.cam.ac.uk (KH)

currently available is less than a few hundred, and this small sample size makes it hard to obtain some statistical properties of distant disc stars. Also, since the errors in distance and proper motion are large, kinematical analyses are difficult for these stars. In the sub-class (ii) studies, much larger sample of stars are available than in the sub-class (i) studies. A recent example of this sub-class is Bovy et al. (2012a), who studied the density distribution of chemically defined disc populations by fitting the SDSS/SEGUE data with analytic models of the density profile. However, since the chemical abundances of these samples are less accurate than high-resolution samples, some blending of the thin- and thick-disc stars is inevitable in this kind of studies. Most of the sub-class (iii) studies are based on the star count method (e.g., Robin et al. 2014). Photometric samples are advantageous in grasping the global structure of the stellar disc because the available sample size is the largest among these sub-classes, and because the sample stars cover a wide range of heliocentric distance. However, since the photometric data lack chemical information for each sample star, it is not possible to separate the sample into stellar components. This inseparability means that one needs to adequately model all the stellar components that contribute to the sample, which is harder than adequately modelling the thick disc only.

By taking into account these problems, in this paper we explore the possibility of constraining the global structure of the thick disc based on a small number of nearby chemically-selected stars, but not relying on analytic modelling of the thick disc. Specifically, we reconstruct the distribution function of the thick disc within a certain portion of the action space which is accessible from local observations.

This paper is organised in the following manner. First, we describe our sample stars in section 2. In section 3, we introduce the concepts of the observable action space $\Gamma_\odot$ and the observable distribution function $f_\odot$. There, we discuss the possibility of inferring some information on the velocity dispersion of the thick disc by using $f_\odot$. In section 4, we present our method to reconstruct $f_\odot$ from a local sample of thick-disc stars. In section 5, we present our main results. The implications from our study are discussed in section 6, and section 7 sums up our analyses.

2   SAMPLE

2.1   The coordinate system and some numerical constants

In this paper, we assume that the Milky Way potential is axisymmetric and adopt the usual Galactocentric cylindrical coordinate system (R, ϕ, z) to describe the three-dimensional positions of stars in the Milky Way. The three-dimensional velocities along the respective coordinates are denoted by (v_R, v_ϕ, v_z), where v_R is positive outwards, v_ϕ is positive in the direction of Galactic rotation, and v_z is positive in the direction of the North Galactic Pole.

We assume that the local standard of rest (LSR) is in a circular orbit with a rotation speed of $v_{\rm LSR} = 240$ km s^{-1} (Reid et al. 2014) and that the Galactocentric distance of the Sun is $R_0 = 8.3$ kpc. We also adopt the peculiar motion of the Sun with respect to the LSR determined by Schönrich et al. (2010).

2.2   Construction of the local thick-disc sample

In this paper, we assume that the thick disc of the Milky Way is a single stellar population and define the thick-disc stars to be those stars with $-1.0 \leqslant {\rm [Fe/H]} \leqslant -0.2$ and ${\rm [Mg/Fe]} \geqslant 0.2$, by taking into account the Solar neighbour observations of disc stars (e.g., Fuhrmann 2011). We constructed a kinematically-unbiased sample of 127 thick-disc stars, for which accurate position, velocity, [Fe/H], and [Mg/Fe] are available. 84 stars in our sample were taken from Adibekyan et al. (2012), and the other 43 stars were taken from Soubiran & Girard (2005). Most of our sample stars are distributed within 100 pc from the Sun.

2.2.1   Sample from Adibekyan et al. (2012)

Adibekyan et al. (2012) published a kinematically-unbiased sample of 1111 stars, for which accurate [Fe/H] and [Mg/H] estimated from high-resolution spectroscopic observations as well as the three dimensional Cartesian velocity based on Hipparcos observations are available. We derived the distances and the line-of-sight velocities for 1103 stars in their sample that were also included in the updated Hipparcos catalog of van Leeuwen (2007). In the course of this inversion, we took into account the Solar peculiar motion adopted in Adibekyan et al. (2012) and we used the three-dimensional Cartesian velocity taken from Adibekyan et al. (2012) and the position on the sky and the proper motion taken from van Leeuwen (2007). We then calculated the three-dimensional velocity (v_R, v_ϕ, v_z) in our coordinate system, by using our assumption on $(R_0, v_{\rm LSR})$. From these 1103 stars, we selected those stars that satisfy both the thick-disc chemical criteria ($-1.0 \leqslant {\rm [Fe/H]} \leqslant -0.2$ and ${\rm [Mg/Fe]} \geqslant 0.2$) and the kinematical criteria of $v_\phi \geqslant 70$ km s^{-1} and $\sqrt{v_R^2 + v_z^2} \leqslant 160$ km s^{-1}. The latter velocity cuts were applied to minimise possible contamination from halo stars. Finally, we discarded those stars that had been flagged as non-single stars, and we obtained 84 stars.

2.2.2   Sample from Soubiran & Girard (2005)

Soubiran & Girard (2005) published a catalog of 743 stars compiled from 11 catalogs of nearby stars and listed the chemical abundances of these stars.[1] Among these 11 catalogs, those catalogs taken from Allende Prieto et al. (2004), Chen et al. (2000), Edvardsson et al. (1993), Mishenina et al. (2004), and Reddy et al. (2003) are kinematically unbiased, so we first selected those stars that are included in either of these five catalogs. Then, we excluded those stars that happened to be included in Adibekyan et al. (2012). The position and velocity of these stars were then calculated either by using the data from Genova-Copenhagen Survey (Holmberg et al. 2009) or by using the updated Hipparcos catalog (van Leeuwen 2007) and SIMBAD database. Finally, as in the previous subsection, we applied the chemical and velocity criteria and obtained 43 thick-disc stars.

---

[1] When more than one published data are available for a certain chemical abundance of a given star, they list the averaged value.
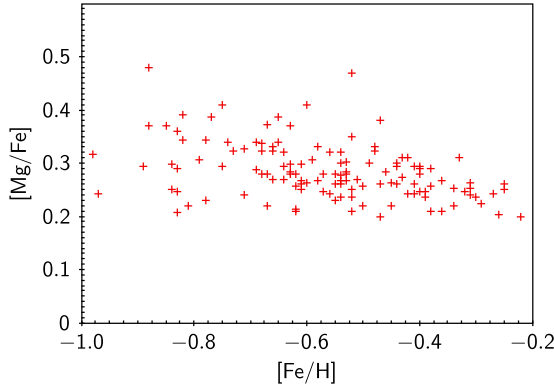
Figure 1. Chemical abundances of our thick-disc sample.

2.2.3   Caveats on the velocity cuts

As described above, we adopted a pair of velocity cuts to exclude halo stars. Rigorously speaking, these cuts potentially could have introduced some kinematical bias on our analyses. However, we have confirmed that adopting a looser velocity constraint of $v_\phi > 0$ km s^{-1} (without cuts on v_R or v_z) has only negligible effects on our final results.

2.3   Chemical and Kinematical properties of our sample

The distribution of our sample stars in the [Fe/H]-[Mg/Fe] plane is shown in Figure 1. The uncertainties in the chemical abundances are small enough (typical uncertainties are Δ[Fe/H] = 0.03 dex and Δ[Mg/Fe] = 0.05 dex for the Adibekyan et al. 2012 sample) compared with the scatter in this diagram. Therefore, our sample does not suffer from severe contamination from low-[Mg/Fe] stars.

Figure 2 shows the velocity distribution of our sample in the (v_ϕ, v_R), (v_ϕ, v_z), (v_R, v_z) and $(v_\phi, \sqrt{v_R^2 + v_z^2})$ planes. Our sample stars show a mean velocity of $(\langle v_R \rangle, \langle v_\phi \rangle, \langle v_z \rangle) = (10.5\pm5.3, 192.3\pm3.6, -7.9\pm3.7)$ km s^{-1}, and thus lag from the LSR by nearly 50 km s^{-1}. The three-dimensional velocity dispersion is $(\sigma_R, \sigma_\phi, \sigma_z) = (59.6, 40.9, 41.6)$ km s^{-1}.

In Figure 3, we show the value of σ_z as functions of v_ϕ and $|v_R|$. To make these plots, we first sort the sample in v_ϕ or $|v_R|$, evaluate the dispersion σ_z for a binned sample of $N = 40$ stars, and move through the sample in steps of 4 stars (so that any pair of adjacent bins share 36 stars). The derived value of σ_z for each bin is plotted against the median value of v_ϕ or $|v_R|$ of the bin.

Although the bin size of 40 stars is rather large compared with the total sample size of 127 stars, the result of this figure suggests that there is no strong trend in σ_z as a function of $|v_R|$ or v_ϕ. This property suggests that the vertical kinematics (σ_z) is not strongly correlated with the in-plane motion ($|v_R|$ or v_ϕ).
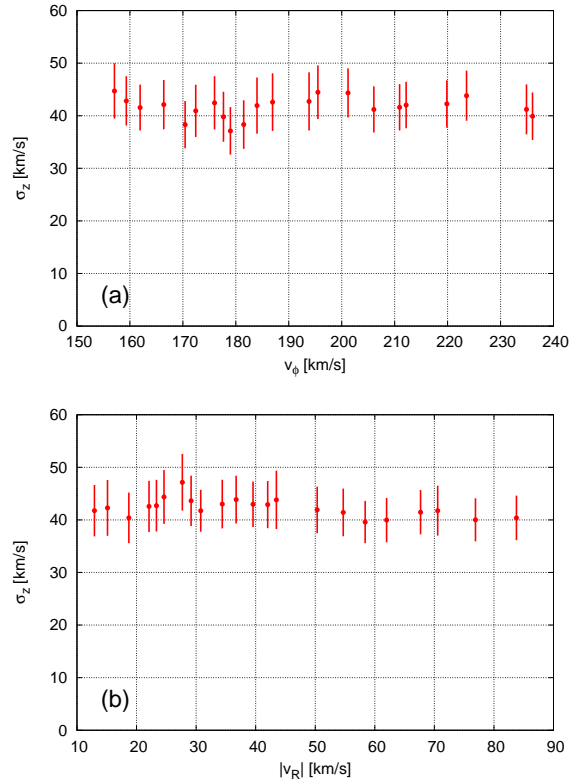

Figure 3. Vertical velocity dispersion σ_z of our thick-disc sample as a function of (a) v_ϕ and (b) $|v_R|$. Each data point represents the value of σ_z of a binned sample of 40 stars, and each pair of adjacent bins share 36 stars in common. The uncertainty in σ_z is calculated by assuming Gaussian distribution of vertical velocity v_z in each bin.

3   THEORY

3.1   Observable distribution function

Most of the thick-disc stars in the Solar neighbourhood are on non-circular orbits. More specifically, the majority of nearby thick-disc stars have guiding radii smaller than the Galactocentric distance of the Sun (R_0), due to the asymmetric drift (Binney & Tremaine 2008). Therefore, if the thick disc is a static stellar system, kinematics of nearby thick-disc stars carry some information on the thick disc outside the Solar neighbourhood, especially on the inner part of the thick disc.

Of course, nearby thick-disc stars do not carry all the information of the thick disc, since these stars are inherently biased in that they represent a portion of the thick-disc stars whose orbits penetrate through the Solar neighbourhood. In other words, a nearby sample only covers a certain fraction of action space $\Gamma_\odot$ where the corresponding orbits bring stars to the Solar neighbourhood (May & Binney 1986). Hence, the best we can do with nearby samples is to reconstruct the distribution function $f(\boldsymbol{J})$ within this *observable action space* $\Gamma_\odot$, i.e. to reconstruct the *observable distribution function* defined by

$$f_\odot(\boldsymbol{J}) = \begin{cases} f(\boldsymbol{J}) & (\boldsymbol{J} \in \Gamma_\odot) \\ 0 & (\text{otherwise}). \end{cases} \qquad (1)$$
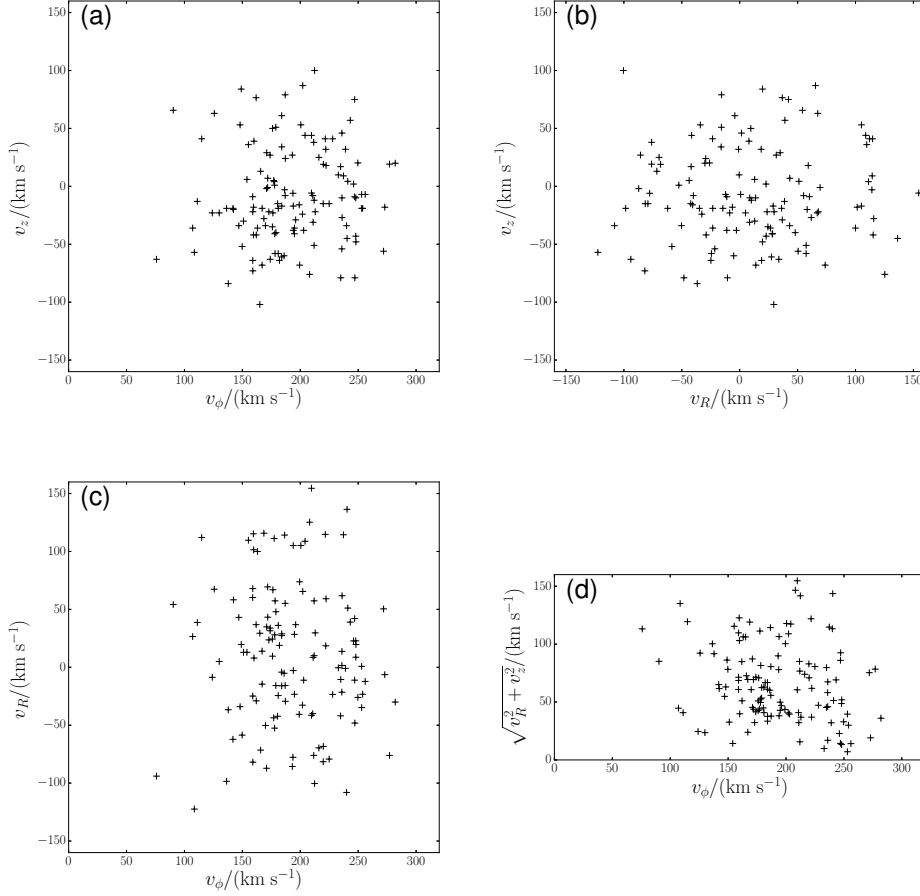
Figure 2. Velocity distributions of our thick-disc sample in (a) (v_ϕ, v_z)-space, (b) (v_R, v_z)-space, (c) (v_ϕ, v_R)-space, and (d) $\left(v_\phi, \sqrt{v_R^2 + v_z^2}\right)$-space.

We here note that $f_\odot(\boldsymbol{J})$ is different from the as-observed action distribution. The fraction of its orbital period that a given star spends in the Solar neighbourhood depends on its orbit, so that the probability of finding the star in the Solar neighbourhood depends on its action. In section 4, we take into account this probability to reconstruct the observable distribution function $f_\odot(\boldsymbol{J})$.

3.2 Observable vertical velocity dispersion

In order to have a physical insight into $\Gamma_\odot$, let us consider the velocity space that corresponds to $\Gamma_\odot$ by assuming a potential model of the Milky Way. Figure 4 shows the allowed range of (v_R, v_ϕ) for disc stars located at $(R, z) = (6, 0)$ kpc with zero vertical velocity to reach the Solar neighbourhood. Since only a portion of the disc stars at $R = 6$ kpc can reach the Solar neighbourhood, what we can learn from $f_\odot$ about the thick disc at $R = 6$ kpc is the velocity distribution of stars within the 'observable' region in Figure 4.

With the information on $f_\odot$, we can estimate the *ob-servable vertical velocity dispersion* defined by

$$\sigma_{z,\odot}^2(R,0) \equiv \frac{\int d^3\boldsymbol{v}\ v_z^2 f_\odot(\boldsymbol{J})}{\int d^3\boldsymbol{v}\ f_\odot(\boldsymbol{J})} \qquad (2)$$

at any given radius R on the disc plane. This dispersion corresponds to the vertical velocity dispersion of those stars located at R whose velocities are within the observable region. Thus $\sigma_{z,\odot}$ is conceptually different from the (ordinary) vertical velocity dispersion given by

$$\sigma_z^2(R,0) = \frac{\int d^3\boldsymbol{v}\ v_z^2 f(\boldsymbol{J})}{\int d^3\boldsymbol{v}\ f(\boldsymbol{J})}, \qquad (3)$$

which is the vertical velocity dispersion of all the stars located at R.

4 METHOD

Here we describe how to reconstruct $f_\odot(\boldsymbol{J})$ of the thick disc from a nearby sample of thick-disc stars, based on the idea of Sommer-Larsen & Zhen (1990). We note that McMillan & Binney (2012) investigated a rigorous treatment of an as-observed distribution function in which survey selection function is taken into account (see Appendix). We
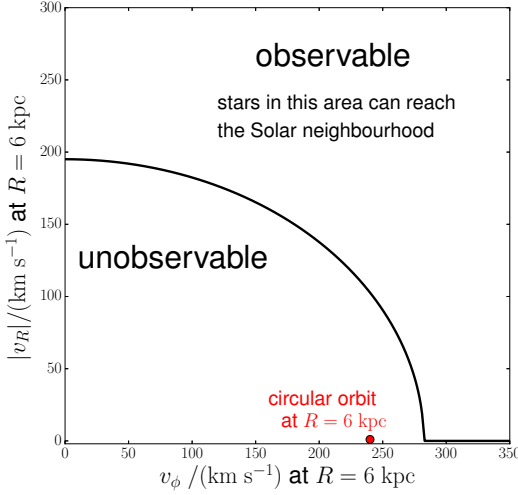
Figure 4. The allowed region in the (v_R, v_ϕ)-space for disc stars at $(R, z) = (6, 0)$ kpc with $v_z = 0$ km s^{-1} to reach the Solar neighbourhood, calculated for the potential model in 5. The boundary curve between the observable region and unobservable region corresponds to $R_{\rm apo} = R_0 = 8.3$ kpc ($R_{\rm apo}$ is the apocentric distance of the orbit), and thus the circular orbit at $R = 6$ kpc (red dot) lies within the unobservable region. When $|v_z| > 0$ km s^{-1}, the boundary curve slightly shifts downwards in this diagram. However, this difference is not significant for a typical value of $|v_z|$ of the thick-disc stars. In this plot, we assume a realistic potential model of the Milky Way described in section 5.

do not follow their formulation here since we do not know the exact survey selection function for our sample stars (but we do know that our sample stars are not kinematically selected). Although we do not take into account the survey selection function, our approach has an advantage that we do not have to assume the functional form of the distribution function.

4.1 Reconstruction of observable distribution function $f_\odot$ of the thick disc

In the following, we regard disc stars as test particles moving in the Milky Way potential. Also, we assume that we have a kinematically-unbiased sample of N thick-disc stars which happen to be passing near the Sun.

Under an axisymmetric potential $\Phi(R, z)$, each star has three actions $\boldsymbol{J} = (J_R, J_\phi, J_z)$ (Binney & Tremaine 2008; Binney 2010). Let us denote the actions of the ith star as $\boldsymbol{J}_i$. Then, the time-averaged distribution function of a single orbit characterised by $\boldsymbol{J}_i$ is expressed as

$$f_i^{\rm single}(\boldsymbol{x}, \boldsymbol{v}) = \frac{1}{(2\pi)^3}\delta(\boldsymbol{J}(\boldsymbol{x}, \boldsymbol{v}) - \boldsymbol{J}_i), \qquad (4)$$

and the corresponding spatial density is given by

$$\rho(\boldsymbol{J}_i; \boldsymbol{x}) = \int d^3\boldsymbol{v}\, f_i^{\rm single} = \frac{1}{(2\pi)^3}\left|\frac{\partial \boldsymbol{v}}{\partial \boldsymbol{J}}\right|_{(\boldsymbol{J}_i, \boldsymbol{x})}. \qquad (5)$$

The value of $\rho(\boldsymbol{J}_i; \boldsymbol{x})$ can be interpreted as the probability density of finding a star with action $\boldsymbol{J}_i$ at position $\boldsymbol{x}$, since $\int d^3\boldsymbol{x} d^3\boldsymbol{v}\, f_i^{\rm single} = 1$ (Chiba & Beers 2001).

By following Sommer-Larsen & Zhen (1990), we approximate the observable distribution function $f_\odot$ to be the weighted sum of single orbit distribution functions given by

$$f_\odot(\boldsymbol{J}) = \sum_{i=1}^N s_i w_i f_i^{\rm single}(\boldsymbol{x}, \boldsymbol{v}). \qquad (6)$$

Here, s_i is a selection index that determines whether the ith star should be included ($s_i = 1$) or not ($s_i = 0$), which shall be introduced to stabilise our analyses. The factor $w_i(> 0)$ is the orbit weighting factor to be determined. Although Sommer-Larsen & Zhen (1990) evaluated w_i through Bayesian statistics, here we numerically evaluate $\rho(\boldsymbol{J}_i; \boldsymbol{x}_i)$ and simply set $w_i = 1/\rho(\boldsymbol{J}_i; \boldsymbol{x}_i)$. This simple choice of w_i corresponds to a limiting case where all of our sample stars have identical position (Sommer-Larsen & Zhen 1990).[2] Since most of our sample stars are located within 100 pc away from the Sun, our simple choice of w_i is well justified.

4.2 Reconstruction of vertical velocity dispersion of the thick disc

Once $f_\odot$ is reconstructed, we can estimate the observable vertical velocity dispersion $\sigma_{z,\odot}$ at a given point on the disc plane, by using equation (2). It can be shown that $\sigma_{z,\odot}(R_0, 0) = \sigma_z(R_0, 0)$ if the assumed potential is correct and a large enough number of local sample stars are available. Thus, we can perform a sanity check of the adopted potential by seeing if these dispersions reasonably agree with each other.

5 ANALYSIS AND RESULTS

5.1 Analysis: Derivation of weighting factors

We adopt a realistic potential model of the Milky Way, consisting of halo, bulge, and disc components.

In our model, the halo potential is given by the Navarro-Frenk-White potential (Navarro et al. 1996) of the form

$$\Phi_{\rm halo} = -v_{\rm H}^2 \frac{\ln(1 + r/d_{\rm H})}{r/d_{\rm H}}, \qquad (7)$$

where r is the Galactocentric distance, $v_{\rm H} = 379.79$ km s^{-1}, and $d_{\rm H} = 9.1$ kpc. The bulge potential is given by

$$\Phi_{\rm bulge} = -\frac{GM_{\rm B}}{c_{\rm B} + r} \qquad (8)$$

(Hernquist 1990). We adopt $M_{\rm B} = 2.05 \times 10^{10} M_\odot$ and $c_{\rm B} = 2$ kpc. We have confirmed that adopting a slightly flattened bulge potential hardly affects our results. For the disc potential, we assume the Miyamoto-Nagai potential (Miyamoto & Nagai 1975) given by

$$\Phi_{\rm discMN} = -\frac{GM_{\rm D}}{\sqrt{R^2 + \left(R_{\rm D} + \sqrt{z^2 + z_{\rm D}^2}\right)^2}} \qquad (9)$$

---

[2] This property can be intuitively understood in the following manner. The probability p of finding a given star in the Solar neighbourhood is equal to the fraction of its orbital period to stay in the Solar neighbourhood. Thus, if such a star is observed in the Solar neighbourhood, it represents $1/p$ stars in the same orbit (including those with different orbital phases).

where $M_D = 5.77 \times 10^{10} M_\odot$, $R_D = 3.2$ kpc, and $z_D = 0.23$ kpc. The values of parameters are chosen by using the publicly available[3] code of `galpy` (Bovy 2015), while fixing $R_0 = 8.3$ kpc, $v_{LSR} = 240$ km s^{-1}, and $c_B = 2$ kpc.

After setting up the potential models, we derived the weighting factor for the ith star, w_i, in the following manner. We first integrated the orbit of the ith star forward in time for a long enough period. We then calculated the fraction δf of the integration time which the star spent in a volume defined by $R_i - \delta R < R < R_i + \delta R$, $z_i - \delta z < z < z_i + \delta z$, and $0 \leqslant \phi < 2\pi$. Here, we denote the observed position of the ith star on the meridional plane as (R_i, z_i) and we adopted $(\delta R, \delta z) = (0.05, 0.1)$ kpc. By taking into account the relation $\delta f = \rho(\boldsymbol{I}_i; \boldsymbol{x}_i) \times 8\pi R_i \delta R \delta z$, we derived $\rho(\boldsymbol{I}_i; \boldsymbol{x}_i)$ and set $w_i = 1/\rho(\boldsymbol{I}_i; \boldsymbol{x}_i)$. We set $s_i = 0$ for those stars that satisfy $w_i > \langle\{w_j\}\rangle + 3\sigma_{\{w_j\}}$, where $\langle\{w_j\}\rangle$ and $\sigma_{\{w_j\}}$ are the mean and the standard deviation of $\{w_j\}$, respectively. This final procedure was included to prevent our results being affected by small number of stars with large w_i.

5.2 Reconstructed vertical velocity dispersion

Figure 5 shows the reconstructed profile of $\sigma_{z,\odot}$. Here we use an approximation of

$$\sigma_{z,\odot}^2(R,0) \simeq \frac{\sum_i s_i w_i \int_0^{\Delta z} dz \int_{R-\Delta R}^{R+\Delta R} dR' \, 2\pi R' \int d^3\boldsymbol{v} \, v_z^2 f_i^{single}}{\sum_i s_i w_i \int_0^{\Delta z} dz \int_{R-\Delta R}^{R+\Delta R} dR' \, 2\pi R' \int d^3\boldsymbol{v} \, f_i^{single}}.$$

(10)

We adopt $(\Delta R, \Delta z) = (0.25, 0.1)$ kpc and calculate $\sigma_{z,\odot}(R,0)$ at $4.5 \leqslant R/\text{kpc} \leqslant 9.5$ in steps of 0.5 kpc. The radial range of R is set so that more than 42 stars (i.e., more than $N/3$ stars) have non-zero contribution to the integrals in equation (10), i,e., have positive values of $\left(s_i \int_{R-\Delta R}^{R+\Delta R} dR' \, 2\pi R' \int d^3\boldsymbol{v} \, f_i^{single}\right)$.

In Figure 5, the red dots show the reconstructed values of $\sigma_{z,\odot}(R,0)$, and the shaded region represents the uncertainty which is derived from a bootstrap resampling of the contributing stars. The velocity dispersion declines nearly exponentially as a function of R, and the best fit exponential profile of $\sigma_{z,\odot}$ is shown with a black straight line. We find that the best-fit scale length defined by

$$R_s \equiv -\left(\frac{d \ln \sigma_{z,\odot}(R,0)}{d R}\right)^{-1}$$

(11)

is $R_s = 8.3 \pm 1.1(\text{rand.}) \pm 1.6(\text{sys.})$ kpc. The random error is the uncertainty in the fit and the systematic error is estimated by performing mock catalog analyses.

We interpolate the values of $\sigma_{z,\odot}$ at $R = 8.0$ kpc and $R = 8.5$ kpc to obtain $\sigma_{z,\odot}(R_0, 0) = 39.4 \pm 2.5$ km s^{-1}. This value is in agreement with the local value of $\sigma_z = 41.6$ km s^{-1} in our sample, indicating that the adopted potential is reasonable at least in the Solar neighbourhood.

5.2.1 Dependency on the adopted potential parameters

We vary the parameters (R_D, z_D) within the range of $2 < R_D/\text{kpc} < 4$ and $0.15 < z_D/\text{kpc} < 0.5$ and find that the
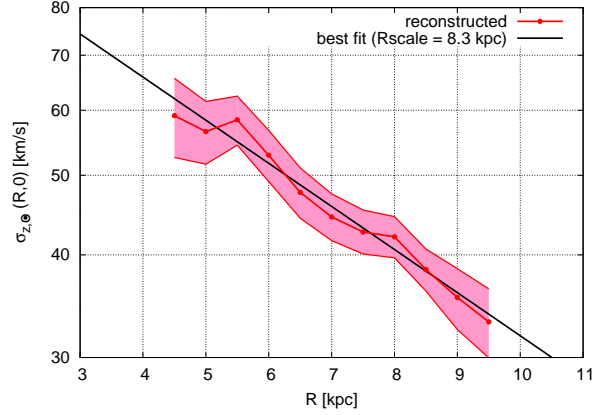
---

[3] Available at http://github.com/jobovy/galpy.

Figure 5. The reconstructed observable vertical velocity dispersion $\sigma_{z,\odot}$ of the thick disc as a function of R.

nearly exponential profile of $\sigma_{z,\odot}$ is a generic feature independent of the assumed parameters. R_s mildly depends on these parameters, but it only increases from 7.5 kpc to 9.4 kpc when we vary R_D from 2 kpc to 4 kpc; and from 8.1 kpc to 9.1 kpc when we vary z_D from 0.15 kpc to 0.5 kpc.

5.3 Dependence of the vertical kinematics on v_R and v_ϕ

As discussed in section 3.2, $\sigma_{z,\odot}(R,0)$ represents the vertical velocity dispersion of stars located at $(R,0)$ whose velocity is within the observable region in the velocity space (Figure 4). In order to see the variation of the vertical kinematics within the observable region, we create the following groups of stars from our sample: (1) those stars with $5.5 < R_{peri}/\text{kpc} < 6.5$ ($N = 26$ stars); and (2) those stars with $5.5 < (1/2)(R_{peri} + R_{apo})/\text{kpc} < 6.5$ ($N = 30$ stars). Here, we define R_{peri} and R_{apo} as the minimum and maximum value of R for each star's orbit. These samples happen to be non-overlapping, and the observed vertical velocity dispersion for groups 1 and 2 are respectively 38.9 ± 5.4 km s^{-1} and 42.6 ± 5.5 km s^{-1}. All of these stars spend some time at $(R, z) = (6.5, 0)$ kpc, so in Figure 6(a), we show the distribution of $|v_R|$ and v_ϕ when they pass through this location. The stars in groups 1 and 2 are distributed in distinct areas in this velocity space, reflecting the different orbital eccentricities. In Figure 6(b), we show the vertical velocity dispersion $\sigma_{z,\odot}(R,0)$ of these groups, calculated by using $\{w_i\}$ derived in section 5. We see that the radial profiles of $\sigma_{z,\odot}(R,0)$ for these groups are quite similar to each other at $6 \leqslant R/\text{kpc} \leqslant 8.5$. This result suggests that the vertical kinematics of the stars in the observable region is more or less homogeneous at least at $6 \leqslant R/\text{kpc} \leqslant 8.5$.

6 DISCUSSION

6.1 Dependency of the vertical kinematics on radial and azimuthal velocities

As seen in Figures 2(a), 2(b), and 3, the vertical velocity dispersion of the thick disc does not have a strong dependency on the in-plane velocities (v_R and v_ϕ) in the Solar
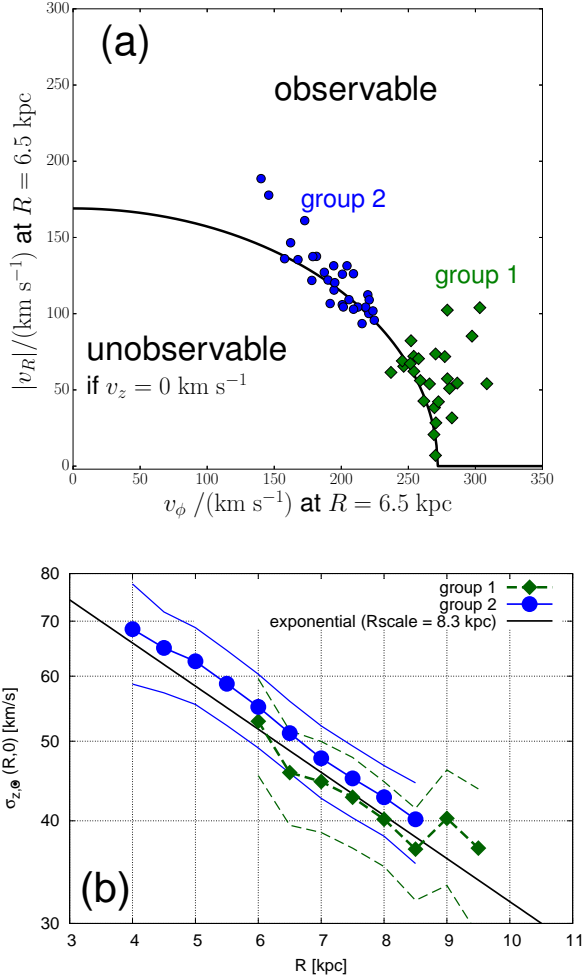
Figure 6. (a) The distribution of stars in group 1 $(5.5 < R_{\rm peri}/{\rm kpc} < 6.5)$ and group 2 $(5.5 < (1/2)(R_{\rm peri} + R_{\rm apo})/{\rm kpc} < 6.5)$ in the $(v_\phi, |v_R|)$ plane when they pass through $(R,z) = (6.5, 0)$ kpc. (b) The reconstructed profile of $\sigma_{z,\odot}$ for these groups. As a reference, we show the exponential profile shown in Figure 5 (black solid line).
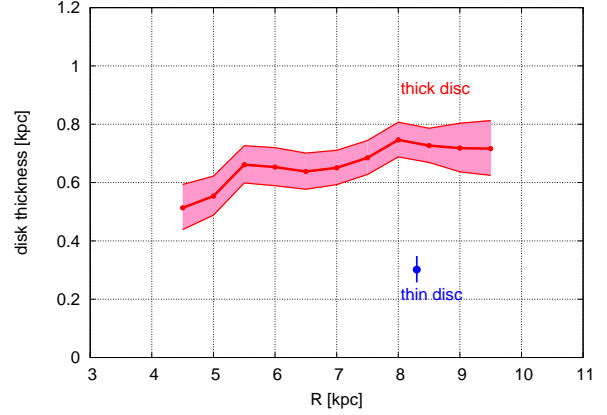

Figure 7. The kinematically-estimated thickness of the thick disc as a function of R by assuming $\sigma_z(R,0) = \sigma_{z,\odot}(R,0)$. Also shown is the kinematically-estimated thickness of the local thin disc which is calculated by assuming $\sigma_z^{\rm thin} = 20 \pm 2.5$ km s^{-1}.

neighbourhood. In order to have some physical insight into this finding, let us suppose, as a working hypothesis, that this apparent homogeneity of vertical velocity distribution across the (v_R, v_ϕ)-space is the case not only near the Sun but also outside the Solar vicinity. Then it is implied that the distribution of the vertical action J_z is not strongly dependent on the radial action (J_R) or azimuthal action (J_ϕ). It follows that there is a typical value of vertical action $J_{z,\rm typical}$ that characterises the vertical motions of the thick-disc stars. On the other hand, the maximum height $z_{\rm max}$ above the disc plane that a given thick-disc star can reach at Galactocentric radius R is determined mainly by its vertical action J_z. In realistic potential models of the Milky Way, $z_{\rm max} \simeq z_{\rm max}(J_z, R)$ is an increasing function of R, since the gravitational pull towards the disc plane is weaker at larger R. Thus, if the distribution of J_z of the thick-disc stars is nearly independent of (J_R, J_ϕ), then the thick disc

needs to flare and the scale height of the thick disc roughly follows the radial behaviour of $z_{\rm max}(J_{z,\rm typical}, R)$.

Then, under what circumstances does the distribution of J_z become (approximately) independent of (J_R, J_ϕ)? Here we consider such an example. Let us suppose that the thick disc was formed through radial migration (Sellwood & Binney 2002; Roškar et al. 2008; Schönrich & Binney 2009a,b; Loebman et al. 2011). Some numerical simulations suggest that the radial migration conserves the stellar vertical action J_z as the star changes its in-plane motion (Solway et al. 2012). Thus, radial migration redistributes the stars in (J_R, J_ϕ)-space while keeping J_z unchanged. This redistribution in the action space is expected to erase the initial dependency of J_z-distribution on (J_R, J_ϕ) (Minchev et al. 2012), unless the initial dependency is too strong to erase. If we take into account that the thick-disc stars are generally very old ($\gtrsim 8$ Gyr; Haywood et al. 2013), it may be likely that the radial migration ends up with a homogeneous distribution of J_z as a function of J_R or J_ϕ. It is of interest to note that some numerical simulations predict that the thick disc flares if it was formed though radial migration (Loebman et al. 2011; Minchev et al. 2012; Roškar et al. 2013).

If σ_z is really independent of (v_R, v_ϕ) anywhere on the disc plane, we have $\sigma_z(R,0) \simeq \sigma_{z,\odot}(R,0)$. In this case we can estimate the thickness $H(R)$ of the thick disc at Galactocentric radius R by using our reconstructed profile of $\sigma_{z,\odot}$. As an example, we define the thickness H by

$$\Phi(R, H(R)) = \Phi(R, 0) + \frac{1}{2}\sigma_z^2(R, 0), \qquad (12)$$

where $\Phi(R, z)$ is the Galactic potential. By plugging $\sigma_{z,\odot}$ into σ_z in equation (12), we obtain $H(R)$ shown in Figure 7. Although the $H(R)$ profile mildly depends on the adopted potential, we have confirmed that H increases as a function of R independent of the potential parameters as long as they are within the range explored in section 5.2.1.

6.2 How can we keep the scale height constant?

As we have discussed in the previous subsection, the radial dependence of the thickness of the thick disc is related to

the dependency of the vertical kinematics on the in-plane motions.

By taking into account some observational evidence of the thick-disc component in external galaxies with a constant scale height (van der Kruit & Searle 1981; Jensen & Thuan 1982; Comerón et al. 2011), let us consider what we would need to keep the scale height H constant. Here we concentrate our discussion on the situation at a certain radius $R = R_1$ in the inner disc ($R_1 < R_0$). In order to satisfy $H(R_1) = H(R_0)$, we require $\sigma_z(R_1, 0) > \sigma_{z,\odot}(R_1, 0)$ so that the vertical velocity distribution is inhomogeneous in the (v_R, v_ϕ) space. Since $\sigma_{z,\odot}$ represents the vertical velocity distribution of observable stars (those stars whose velocity is inside the observable region) and σ_z represents the vertical velocity distribution of all the stars, this requirement implies the following situation: In the inner disc, those thick-disc stars with large J_ϕ (large guiding centre radii) need to have smaller vertical action than those thick-disc stars with small J_ϕ and J_R.[4] This situation may be attained if there are enough low-eccentricity, shell-like orbits with large vertical motions in the inner disc.

7   CONCLUSIONS

We have investigated an orbit-based method to reconstruct the observable distribution function $f_\odot$, which describes the distribution of action within the portion of action space covered by a local disc sample. By applying our method to 127 chemically-selected thick-disc stars in the Solar neighbourhood, we found that the vertical velocity dispersion $\sigma_{z,\odot}$ that corresponds to $f_\odot$ decreases nearly exponentially as a function of R with a scale length of $R_s = 8.3 \pm 1.1(\text{rand.}) \pm 1.6(\text{sys.})$ kpc.

We also found that the vertical velocity dispersion σ_z of the local thick-disc stars shows only weak dependency on the in-plane motions (v_R, v_ϕ). This apparent homogeneity of σ_z in (v_R, v_ϕ)-space may be naturally explained if the distribution of the vertical action J_z is only weakly dependent on the radial action J_R and the azimuthal angular momentum J_ϕ. One possible mechanism to produce such action distribution is radial migration, where the thick-disc stars are re-distributed in the (J_R, J_ϕ)-space while keeping their J_z unchanged (Minchev et al. 2012).

---

[4] In order for a given star at $R = R_1 < R_0$ with small J_ϕ to be unobservable, it has to have small $|v_R|$ (see Figure 4) and thus small J_R.

REFERENCES

Adibekyan, V. Z., Sousa, S. G., Santos, N. C., et al. 2012, A&A, 545, A32

Allende Prieto, C., Barklem, P. S., Lambert, D. L., & Cunha, K. 2004, A&A, 420, 183

Bensby, T., Feltzing, S., & Lundström, I. 2003, A&A, 410, 527

Bensby, T., Feltzing, S., & Lundström, I. 2004, A&A, 415, 155

Bensby, T., Alves-Brito, A., Oey, M. S., Yong, D., & Meléndez, J. 2011, ApJ, 735, L46

Binney, J. 2010, MNRAS, 401, 2318

Binney, J. 2012, MNRAS, 426, 1328

Binney, J., & McMillan, P. 2011, MNRAS, 413, 1889

Binney, J., & Tremaine, S. 2008, Galactic Dynamics: Second Edition, by James Binney and Scott Tremaine. ISBN 978-0-691-13026-2 (HB). Published by Princeton University Press, Princeton, NJ USA, 2008.

Bovy, J., Rix, H.-W., Liu, C., et al. 2012, ApJ, 753, 148

Bovy, J., & Rix, H.-W. 2013, ApJ, 779, 115

Bovy, J. 2015, ApJS, 216, 29

Brook, C. B., Kawata, D., Gibson, B. K., & Freeman, K. C. 2004, ApJ, 612, 894

Brook, C. B., Gibson, B. K., Martel, H., & Kawata, D. 2005, ApJ, 630, 298

Chen, Y. Q., Nissen, P. E., Zhao, G., Zhang, H. W., & Benoni, T. 2000, A&AS, 141, 491

Chiba, M., & Beers, T. C. 2001, ApJ, 549, 325

Comerón, S., Elmegreen, B. G., Knapen, J. H., et al. 2011, ApJ, 741, 28

Edvardsson, B., Andersen, J., Gustafsson, B., et al. 1993, A&A, 275, 101

Fuhrmann, K. 1998, A&A, 338, 161

Fuhrmann, K. 2004, Astronomische Nachrichten, 325, 3

Fuhrmann, K. 2008, MNRAS, 384, 173

Fuhrmann, K. 2011, MNRAS, 414, 2893

Gilmore, G., & Reid, N. 1983, MNRAS, 202, 1025

Gilmore, G., Wyse, R. F. G., & Kuijken, K. 1989, ARA&A, 27, 555

Haywood, M., Di Matteo, P., Lehnert, M. D., Katz, D., & Gómez, A. 2013, A&A, 560, A109

Hernquist, L. 1990, ApJ, 356, 359

Holmberg, J., Nordström, B., & Andersen, J. 2009, A&A, 501, 941

Jensen, E. B., & Thuan, T. X. 1982, ApJS, 50, 421

Kuijken, K., & Gilmore, G. 1989, MNRAS, 239, 571

Loebman, S. R., Roškar, R., Debattista, V. P., et al. 2011, ApJ, 737, 8

Masseron, T., & Gilmore, G. 2015, arXiv:1503.00537

McMillan, P. J., & Binney, J. 2012, MNRAS, 419, 2251

May, A., & Binney, J. 1986, MNRAS, 221, 857

Minchev, I., Famaey, B., Quillen, A. C., et al. 2012, A&A, 548, A127

Mishenina, T. V., Soubiran, C., Kovtyukh, V. V., & Korotin, S. A. 2004, A&A, 418, 551

Miyamoto, M., & Nagai, R. 1975, PASJ, 27, 533

Navarro, J. F., Frenk, C. S., & White, S. D. M. 1996, ApJ, 462, 563

Reddy, B. E., Tomkin, J., Lambert, D. L., & Allende Prieto, C. 2003, MNRAS, 340, 304

Reddy, B. E., Lambert, D. L., & Allende Prieto, C. 2006,

MNRAS, 367, 1329

Reid, M. J., Menten, K. M., Brunthaler, A., et al. 2014, ApJ, 783, 130

Rix, H.-W., & Bovy, J. 2013, A&A Rev., 21, 61

Roškar, R., Debattista, V. P., Stinson, G. S., et al. 2008, ApJ, 675, L65

Roškar, R., Debattista, V. P., & Loebman, S. R. 2013, MNRAS, 433, 976

Robin, A. C., Reylé, C., Fliri, J., et al. 2014, A&A, 569, AA13

Sanders, J. L., & Binney, J. 2015, MNRAS, 449, 3479

Sellwood, J. A., & Binney, J. J. 2002, MNRAS, 336, 785

Schönrich, R., & Binney, J. 2009, MNRAS, 396, 203

Schönrich, R., & Binney, J. 2009, MNRAS, 399, 1145

Schönrich, R., Binney, J., & Dehnen, W. 2010, MNRAS, 403, 1829

Solway, M., Sellwood, J. A., & Schönrich, R. 2012, MNRAS, 422, 1363

Sommer-Larsen, J., & Zhen, C. 1990, MNRAS, 242, 10

Soubiran, C., & Girard, P. 2005, A&A, 438, 139

van der Kruit, P. C., & Searle, L. 1981, A&A, 95, 105

van Leeuwen, F. 2007, A&A, 474, 653

Yoshii, Y. 1982, PASJ, 34, 365

Yoshii, Y. 2013, Planets, Stars and Stellar Systems. Volume 5: Galactic Structure and Stellar Populations, 393

APPENDIX A: SELECTION FUNCTION OF THE SURVEY

In our analyses, we followed the approach of Sommer-Larsen & Zhen (1990) to relate the observed kinematic data to the underlying distribution function. We note here that our approach owes much to the fact that our sample stars are located at the immediate Solar neighbourhood ($d \lesssim 100$ pc).

Let us consider a sample of stars taken from an imaginary magnitude-limited survey in which all the stars with apparent magnitude brighter than a certain value are observed. In this case, those sample stars at large distances are high-luminosity stars, while the sample covers a wider luminosity range for nearby stars. Thus, such a sample puts more weight on nearby stars. If the kinematical properties are highly inhomogeneous within the surveyed region, this sample is kinematically biased. In general, if the surveyed region is large, the survey selection function has to be taken into account in order to estimate the kinematic properties of the system (McMillan & Binney 2012). This means that our methodology is not applicable to a sample that covers a large volume unless the completeness is taken into account, since our method implicitly requires that the sample stars are fair representatives of the stellar population. However, since our sample is distributed in a small region ($d \lesssim 100$ pc), it is safe to assume that the kinematical properties of the thick-disc stars are homogeneous inside this region (the thick disc has a scale height of ~ 1 kpc and a scale length of 2-3 kpc). Therefore, the effect from the (poorly-known) survey selection function is relatively small in our sample.